

Locally Optimally Emitting Clouds and the Origin of Quasar Emission Lines

Jack Baldwin

Cerro Tololo Interamerican Observatory¹, Casilla 603, La Serena, Chile

Gary Ferland, Kirk Korista, and Dima Verner

Department of Physics & Astronomy, University of Kentucky, Lexington, KY 40506

ABSTRACT

The similarity of quasar line spectra has been taken as an indication that the emission line clouds have preferred parameters, suggesting that the environment is subject to a fine tuning process. We show here that the observed spectrum is a natural consequence of powerful selection effects. We computed a large grid of photoionization models covering the widest possible range of cloud gas density and distance from the central continuum source. For each line only a narrow range of density and distance from the continuum source results in maximum reprocessing efficiency, corresponding to “locally optimally emitting clouds” (LOC). These parameters depend on the ionization and excitation potentials of the line, and its thermalization density. The mean QSO line spectrum can be reproduced by simply adding together the full family of clouds, with an appropriate covering fraction distribution. The observed quasar spectrum is a natural consequence of the ability of various clouds to reprocess the underlying continuum, and can arise in a chaotic environment with no preferred pressure, gas density, or ionization parameter.

Subject headings: quasars: emission lines

¹Operated by the Association of Universities for Research in Astronomy Inc. (AURA) under cooperative agreement with the National Science Foundation

1. Introduction

The question of the origin of quasar emission line regions is central to calibrating these objects as probes of the Universe at the epoch of galaxy formation. Once we understand the spectrum in detail there is the potential of measuring their distances (and hence q_0 and H_0) and of determining the composition of the gas, thus constraining nucleosynthesis during galaxy formation.

Although the promise is great, progress has been slow. The lines are produced by a dilute gas far from LTE. Its spectrum is sensitive to line formation details, particularly the cloud gas density and flux of radiation (Netzer 1992). These are often combined into a single “ionization parameter”, the ratio of photon to gas densities. The earliest observations showed that the family of quasars have surprisingly similar emission line spectra (Davidson & Netzer 1979), and this is often taken as evidence that a process adjusts clouds to a certain ionization parameter (Davidson 1977, Krolik, McKee, & Tarter 1981). The possible presence of an unspecified tuning mechanism made it impossible to know how to interpret correlations between emission line parameters and other properties (*e.g.*, Baldwin, Wampler, & Gaskell 1989). Finely tuned cloud parameters suggest a highly ordered environment, not the chaotic one that might naturally result during the initial stages of galaxy formation.

More recent work by Rees, Netzer, & Ferland (1989), Krolik et al. (1991), Goad, O’Brien, & Gondhalekar (1993), and O’Brien, Goad, & Gondhalekar (1994, 1995) have investigated distributed emission line cloud properties, but still assumed the existence of a single cloud pressure law with radius. Here we use a much more general approach to show that a powerful selection effect operates, so that a random mix of cloud properties will produce the spectrum of a typical QSO. There is no spectroscopic evidence for finely tuned cloud parameters. The spectrum of a typical quasar is consistent with spectral formation in an environment with no preferred pressure, gas density, or ionization parameter.

2. A Single Cloud

We model individual clouds using the following assumptions: a single column density of $N(\text{H}) = 10^{23} \text{ cm}^{-2}$, constant hydrogen density throughout each cloud, and solar metallicity. Although below we show results for a single cloud column density, we expect there to be a broad range of column densities present in the BLR. Preliminary investigations into the sensitivity of the results to the presence of a range of column densities indicate that they are not strongly affected as long as optically thin clouds do not dominate the total line emission. With the exception of N V $\lambda 1240$, most of the prominent emission lines are not

strongly affected by our choice of metallicity (see Hamann & Ferland 1993).

The ionizing continuum shape chosen was a combination of a $f_\nu \propto \nu^{-0.3} \exp(-h\nu/kT_{cut})$ UV-bump with an X-ray power law of the form $f_\nu \propto \nu^{-1}$ spanning 13.6 eV to 100 keV. The UV-bump cutoff temperature, T_{cut} , was chosen such that the energy in the UV-bump peaked at 48 eV. The two continuum components were combined using a typical QSO UV to X-ray logarithmic spectral slope of $\alpha_{ox} = -1.4$ (note the explicit minus sign). Korista et al. (1996) will explore in detail the dependencies of the emitted line spectrum on continuum shape, chemical abundances, and cloud column density.

The remaining parameters are the cloud particle density $n(H)$ (cm^{-3}) and the photon flux of H-ionizing radiation $\Phi(H)$ ($\text{cm}^{-2} \text{ s}^{-1}$). For an isotropic continuum source $\Phi(H)$ is a direct measure of the distance between the clouds and the continuum source r . The variables r and $n(H)$ directly describe the overall structure of the BLR, and we do not combine them into an ionization parameter $U(H) = \Phi(H)/n(H)c$.

3. Locally Optimally-emitting Clouds (LOC)

Figure 1 shows the results of a large series of photoionization calculations in which $\Phi(H)$ and $n(H)$ were varied. Lines are presented as equivalent widths for full geometrical coverage, referred to the incident continuum at 1215 Å. This equivalent width is a direct measure of the cloud’s reprocessing efficiency.

Collisionally excited lines such as C IV $\lambda 1549$ show a band of efficient reprocessing running at constant $U(H)$ along a diagonal ridge from high $\Phi(H)$ and $n(H)$, to low $\Phi(H)$ and $n(H)$. Along this ridge, corresponding to $\log U(H) \approx -1.5$ for $\lambda 1549$, the gentle decrease in the W_λ at the high densities is caused by line thermalization — high density clouds are continuum sources. The line equivalent width decreases sharply when moving orthogonal to the ridge because $U(H)$ is either too low (lower right) or too high (upper left) to produce the line efficiently. Clouds with $\log U(H) \gtrsim 0.2$ are optically thin so reprocess little of the incident continuum. C IV can be contrasted with a low ionization line such as Mg II $\lambda 2798$, whose peak W_λ is shifted to lower $U(H)$, or to the high ionization O VI $\lambda 1034$, shifted to higher $U(H)$ (≈ 1). Note that the contours in Figure 1 are logarithmic; in linear space they are sharply peaked. We then see that the line formation radius naturally depends on the ionization potential (IP), modulated by thermalization density; low IP lines form at large radii and high IP at small radii, a result consistent with line-continuum reverberation measurements (Peterson 1993).

Recombination lines of H^o and He⁺ emit over a wider area on the density–flux

plane, including the low $\Phi(H)$ – high $n(H)$ regions since both ions still exist under these conditions. On the whole, Ly α forms closer in than H β . This is because Ly α is a resonance line and is collisionally suppressed at high densities, while H β is suppressed at high flux due to larger excited state optical depths (Ferland, Netzer, & Shields 1979). This will make Ly α respond first to continuum variations and make its line profile broader in the wings if cloud motions are purely virial. The first effect is observed (Clavel et al. 1991; Peterson et al. 1991); the second effect is often but not always observed (Zheng 1992; Netzer et al. 1995). For He II λ 1640, the region of most efficient reprocessing is a diagonal plateau (rather than a ridge), peaking and saturating at high density and flux, but also diminishing at very low ionization parameter. This peak and much of the plateau are at significantly larger flux than for H β , thus λ 1640 is formed in gas lying closer to the continuum source. This is also consistent with the reverberation measurements (Korista et al. 1995).

4. The Integrated LOC Spectrum

The equivalent widths for full coverage, as plotted in Figure 1, represent the efficiency with which the individual LOC clouds can reprocess ionizing continuum radiation into line radiation. These reprocessing efficiencies act as a filter whose output is the QSO’s emission line spectrum. Each line can be formed efficiently only at a particular location in the density–flux plane. This location is different for different lines. If the individual clouds are distributed over a wide range on the density–flux plane, then most emission lines will be produced with high efficiency, so long as that component has a significant covering fraction.

The simplest description of this type of system is to take, for each separate line, the extreme case of considering only emission from a cloud with the optimal density and flux parameters for the line in question. Under these conditions the relative intensity of each emission line would be directly proportional to the maximum reprocessing efficiency, for uniform covering fraction. Column 2 in Table 1 presents a mean observed QSO spectrum, and in column 3 are the results of this simple model. The two are in good agreement.

A more realistic refinement is to assume some distribution of clouds on the density–flux plane and use that as a weighting function to integrate over the distribution of reprocessing efficiencies. The limits of this integration are set by physical or observational considerations: clouds at large distances from the continuum source ($\log \Phi(H) < 18$) will form graphite grains (Sanders et al. 1989) and therefore have very low emissivity (Netzer & Laor 1993); very low density clouds ($n(H) < 10^8 \text{ cm}^{-3}$) are ruled out by the absence of broad forbidden lines, such as [O III] λ 4363. Clouds at very small radii or with very high densities are either at the Compton temperature or are so dense that they are continuum rather than emission

line sources. Thus to produce the emission line spectrum, one simply integrates the line emission from clouds along each axis in Figure 1 ($\log n(H) \geq 8$, $\log \Phi(H) \geq 18$).

Remaining to be specified are the distribution of clouds as functions of distance from the continuum source and gas density, appearing in the definition of the emission line luminosity,

$$L_{line} \propto \iint r^2 F(r) f(r) g(n) dn dr, \quad (1)$$

where $F(r)$ is the emission line flux of a single cloud at radius r , and $f(r)$ and $g(n)$ are the cloud covering fractions with radius and gas density, respectively. Column 4 of Table 1 shows the results for the simple case of $f(r) \propto constant$ and $g(n) \propto n^{-1}$; the results are sensitive to these distributions and will be discussed in Korista et al. (1996). The agreement with the observations again is quite good, with the exception of N V $\lambda 1240$ (underpredicted, as usual for solar abundances, see Hamann and Ferland 1993). Some of the other weaker lines in Table 1 whose predicted relative intensities lie near the bottom of the observed distribution should also be larger in gas of higher metallicity expected in QSOs (*e.g.*, Si III], Si IV, Al III). The $Ly\alpha/H\beta$ ratio is still problematical, with large uncertainties in intrinsic reddening and radiative transfer in the Balmer lines (Netzer et al. 1995). In this example, a total geometrical covering fraction of 18% will produce the typical $W_\lambda(Ly\alpha) = 100 \text{ \AA}$.

5. Conclusions

These results show that line emission from the BLR is dominated by powerful selection effects. Individual BLR clouds can be thought of as just machines for reprocessing radiation. As long as there are enough clouds at the correct radius and with the correct gas density to efficiently form a given line, the line will be formed with a relative strength which turns out to be very similar to the one actually observed. Thus there is no spectroscopic evidence for preferred cloud parameters. Observed QSO spectra carry information mostly about global properties such as the continuum shape, the clouds' overall metallicity, and their distribution, rather than about the details of individual clouds.

This in turn shows that a jumbled or chaotic cloud environment can be the source of the lines. The spectrum of a typical quasar may be produced in a scrambled environment similar to that which might occur in the center of a proto-galaxy, with rapid star formation, evolution, and supernova activity.

A ramification of the fact that lines form at different places is that we can qualitatively reproduce many of the observed variability and line width differences. This picture also provides a natural explanation for why the sizes of the emission line regions scale with

luminosity (Peterson 1993); lines naturally form at the appropriate ionizing fluxes, and the corresponding radii scale with luminosity.

Many aspects of the LOC picture are under investigation: sensitivity of results to ionizing continuum shape, metallicity, cloud covering factor distributions with radius and gas density, resulting line profiles and reverberation. The likely presence of a broad range of cloud column densities converts the LOC plane to a cube ($\Phi(H), n(H), N(H)$).

If the LOC picture proves to be correct then our understanding of the BLR will have undergone the same change as did our view of the Narrow Line Region when it was realized that all of the forbidden lines were radiating near their critical densities (Filippenko & Halpern 1984). Simple averaging, not a hidden hand or unknown physics, is at work.

We are grateful to Mark Bottorff, Moshe Elitzur, and the referee Simon Morris for helpful comments. This work was supported by the NSF (AST 93-19034), NASA (NAGW-3315), and STScI grant GO-2306.

TABLE 1
OBSERVED AND PREDICTED LINE INTENSITIES

Emission Line (1)	Observed Intensity ^a (2)	Maximum Reprocessing (3)	LOC Integration ^b (4)
O VI $\lambda 1034 + \text{Ly}\beta \lambda 1026$	0.1–0.3	0.28	0.16
Ly α $\lambda 1216$	1.00	1.00	1.00
N V $\lambda 1240$	0.1–0.3	0.06	0.04
Si IV $\lambda 1397 + \text{O IV] } \lambda 1402$	0.08–0.24	0.08	0.06
C IV $\lambda 1549$	0.4–0.6	0.54	0.57
He II $\lambda 1640 + \text{O III] } \lambda 1666$	0.09–0.2	0.11	0.14
C III]+Si III]+Al III $\lambda 1900$	0.15–0.3	0.28	0.12
Mg II $\lambda 2798$	0.15–0.3	0.38	0.34
H β $\lambda 4861$	0.07–0.2	0.08	0.09

^aIntensity relative to Ly α $\lambda 1216$, combining data from Baldwin, Wampler, & Gaskell (1989), Boyle (1990), Cristiani & Vio (1990), Francis et al. (1991), Laor et al. 1995, Netzer et al. (1995), and Weymann et al. (1991).

^bCo-addition of emission from clouds as described in the text.

REFERENCES

- Baldwin, J.A., Wampler, E.J., & Gaskell, C.M. 1989, *ApJ*, 338, 630
- Boyle, B.J. 1990, *MNRAS*, 243, 231
- Clavel, J., et al. 1991, *ApJ*, 366, 64
- Cristiani, S., & Vio, R. 1990, *A&A*, 227, 385
- Davidson, K. 1977, *ApJ*, 218, 20
- Davidson, K., & Netzer, H. 1979, *Rep. Prog. in Physics* 51, 715
- Ferland, G.J., Netzer, H., & Shields, G.A. 1979, *ApJ*, 232, 382
- Francis, P., Hewett, P., Foltz, C., Chaffee, F., Weymann, R., & Morris, S. 1991, *ApJ*, 373, 465
- Filippenko, A.V., & Halpern, J.P. 1984, *ApJ*, 285, 458
- Goad, M.R., O'Brien, P.T., & Gondhalekar, P.M. 1993, *MNRAS*, 263, 149
- Hamann, F., & Ferland, G.J. 1993, *ApJ*, 418, 11
- Korista, K.T., et al. 1995, *ApJS*, 97, 285
- Korista, K.T., Baldwin, J.A., and Ferland, G.J. 1996, in preparation
- Krolik, J.H., McKee, C.M., & Tarter, C.B. 1981, *ApJ*, 249, 422
- Krolik, J.H., Horne, K., Kallman, T.R., Malkan, M.A., Edelson, R.A., & Kriss G.A. 1991, *ApJ*, 371, 541
- Laor, A., Bahcall, J., Januzzi, B.T., Schneider, D.P., & Green, R.F. 1995, *ApJ*, in press
- Netzer, H. 1992, in *Active Galactic Nuclei, Saas-Fee Advanced Course 20*, ed. R. Blandford, H. Netzer, & L. Woltjer, (Springer-Verlag), p57
- Netzer, H., Brotherton, M.S., Wills, B.J., Han, M., Wills, D., Baldwin, J.A., Ferland, G.J., & Brown, I.W.A. 1995, *ApJ*, 448, 27
- Netzer, H., & Laor, A. 1993, *ApJ*, 404, L51
- O'Brien, P.T., Goad, M.R., & Gondhalekar, P.M. 1994, *MNRAS*, 268, 845
- O'Brien, P.T., Goad, M.R., & Gondhalekar, P.M. 1995, *MNRAS*, 275, 1125
- Peterson, B.M. 1993, *PASP*, 105, 247
- Peterson, B.M., et al. 1991, *ApJ*, 368, 119
- Rees, M.J., Netzer, H., & Ferland, G.J. 1989, *ApJ*, 347, 640
- Sanders, D.B., et al. 1989, *ApJ*, 347, 29
- Weymann, R.J., Morris, S.L., Foltz, C.B., & Hewett, P.C. 1991, *ApJ*, 373, 23

Zheng, W. 1992, ApJ, 385, 127

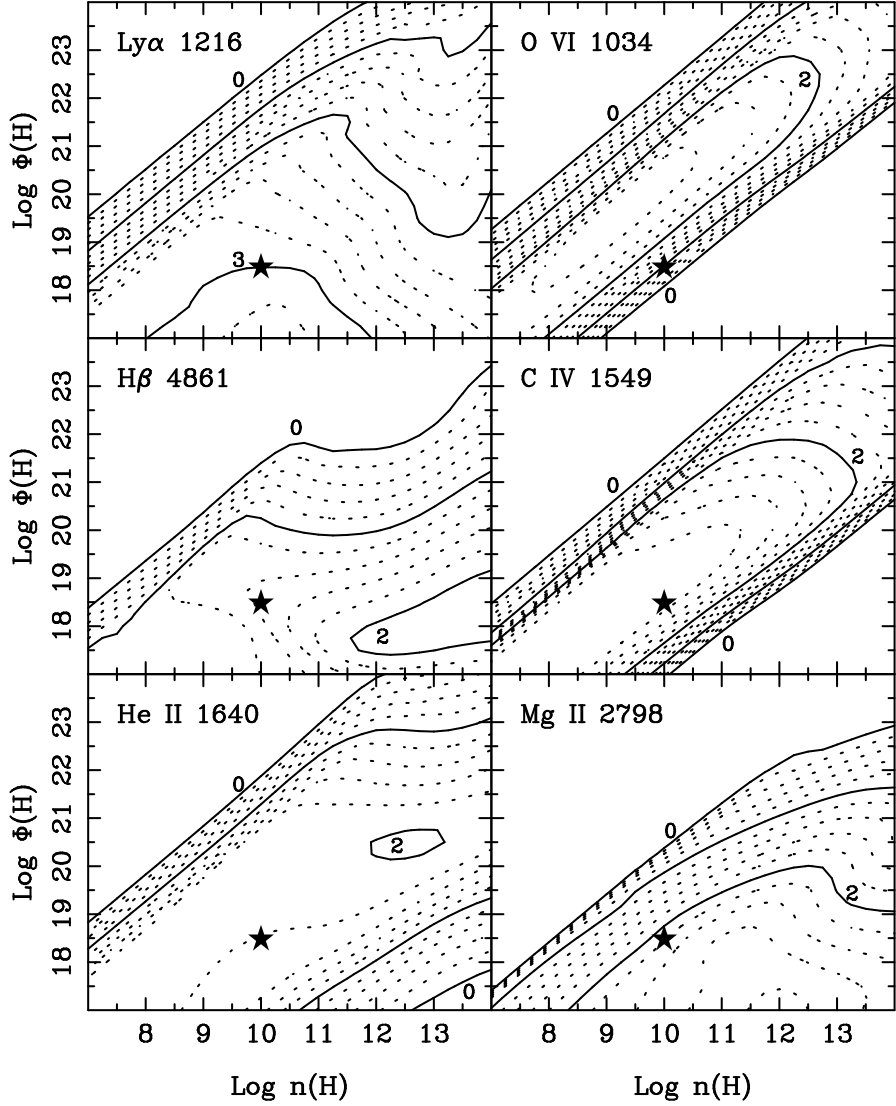


Fig. 1.— Cloud reprocessing efficiency is shown as a function of the hydrogen density and flux of ionizing photons. Line strengths are expressed as equivalent widths referenced to the incident continuum at 1215 Å. Each bold line is 1 dex, and dotted lines represent 0.2 dex steps. The smallest (1 Å) and largest decade contours are labeled for each line; note that the contour values continue to increase beyond the largest labeled decade in all cases but $\text{H}\beta$ and He II. The star is a reference point marking the “standard BLR” parameters discussed by Davidson and Netzer (1979).